Mesenchymal stem cells in skeletal muscle regeneration

Garza-Rodea, A.S. de la

Chapter 6

Regeneration of human skeletal muscle in a mouse model

AS de la Garza-Rodea, H Boersma, C Dambrot, AAF de Vries,
DW van Bekkum, S Knaän-Shanzer

Abstract

Currently, skeletal muscle regeneration and treatment of myodegeneration are mainly studied in animals. The translational relevance of such models is doubtful due to the possible involvement of species-specific factors in skeletal muscle repair. The myoregenerative properties of human stem and precursor cells are thus best studied in human subjects. However, practical and ethical issues greatly limit the possibility to investigate skeletal muscle repair in humans and *in vitro* regeneration of human skeletal muscle tissue has not yet been achieved. Accordingly, in the present study we developed a murine model for comparing the contribution of human and mouse cells to the repair of damaged human or murine skeletal muscle tissue. To this end, minced human or mouse skeletal muscle tissue was implanted subcutaneously in mice with or without human or murine mesenchymal stem cells (hMSCs and mMSCs, respectively).

Skeletal muscle implants with and without MSCs were collected at 7, 15, 30 and 45 days after transplantation and analyzed, using immunohistological methods, for encapsulation, degeneration/regeneration and vascularization.

Regeneration of the implanted fresh muscle tissue was observed as early as day 7 and progressed with time. In general, regeneration proceeded from the periphery of the implant inwards. Human skeletal muscle regeneration lagged clearly behind that of murine skeletal muscle. As we failed to obtain sufficient amounts of fresh human muscle tissue on a regular basis, for most experiments, we had to resort to samples that had been cryopreserved. This appeared, however, to be detrimental to the human satellite cells resulting in defective myoregeneration causing the implants to morphologically resemble skeletal muscle tissue of Duchenne muscular dystrophy (DMD) patients at a late stage of disease. In contrast, regeneration of murine muscle that had been cryopreserved proceeded similarly to that of fresh tissue.

LacZ-tagged hMSCs and mMSCs that had been mixed with the minced muscle prior to implantation were detected early after grafting (day 7, 15) as single cells at the periphery of the implants, where vascularization began. β-galactosidase-positive (β-gal$^+$) myofibers were seen at days 30 and 45 after transplantation in both fresh and cryopreserved mouse muscle implants supplied with mMSCs.

Interestingly, for the combination of hMSCs and minced mouse muscle, hybrid myo-fibers were only observed when the human cells were added to mouse muscle that had been cryopreserved, but not when they were mixed with fresh murine muscle pieces. This observation suggests that murine muscle tissue does not provide an optimal environment for hMSC maintenance and incorporation into myofibers and that their myoregenerative ability may be underestimated in mouse models.

Our preliminary findings with the subcutaneous skeletal muscle implants seem to merit the further development of this model system. Its usefulness will be significantly increased by devising an effective technique for the cryopreservation of satellite cells in human muscle samples.

Introduction

The recent advances in (i) the derivation of human pluripotent stem cells, (ii) the characterization and *ex vivo* amplification of human somatic stem cells and (iii) the genetic modification of these cells have created new prospects for cell-based therapies. The therapeutic potential of (engineered) human stem cells should ideally be validated in humans. Due to practical and ethical concerns this type of studies is, however, largely restricted to animals. Transplantation of different human stem cell types including pericytes[1], satellite cells[1], mesenchymal stem cells (MSCs)[2] and muscle precursor cells[3] into damaged murine skeletal muscle revealed consistently that 1-7% of the myofibers in the regenerated tissue contained human nuclei. Similar experiments performed with murine satellite cells injected into muscles of *mdx* mice[4] showed more than 10% chimeric myofibers after the administration of a significant smaller cell inoculum. The reconstitution frequency by syngeneic donor cells was even more profound in *mdx* mice transplanted with a subpopulation of satellite cells with 94% of all myofibers becoming chimeric[5]. Although these findings require confirmation by direct comparative studies, they suggest a higher propensity of murine than of human (stem) cells to participate in the regeneration of mouse skeletal muscle tissue. Consequently, the results of preclinical studies with human stem cells in mice may lead to an underestimation of their therapeutic potential in man.

The present study is an attempt to develop a method for investigating this assumption. This method is based on the free grafting together with human MSCs (hMSCs) or mouse MSCs (mMSCs) of minced human or mouse skeletal muscle tissue in the subcutis of mice. Successful free grafting of mammalian muscles was first accomplished in the 1960s[6]. As implants either intact or minced skeletal muscle pieces have been used. Transplantation of these materials occurred into an emptied skeletal muscle bed or at a heterotopic anatomical site[7-10]. Under all conditions, myoregeneration was preceded by host-mediated vascularization and innervation[6,8,22] of the grafted tissue. We selected the subcutis as site of implantation for convenience and to preclude participation of host muscle cells in the regeneration of the graft[7-9]. The main reason to work with minced tissue was that it can be easily and homogenously mixed prior to implantation with the stem cells under investigation. As recipient of allogeneic and xenogeneic transplants we used non-obese diabetic/severe combined immunodeficient (NOD/SCID) mice to prevent their immune rejection.

Materials and Methods

Skeletal muscle tissues

Human skeletal muscle specimens were left over from orthopedic surgery obtained according to the guidelines of the Leiden University Medical Center (LUMC, Leiden, the Netherlands). The samples were washed once with phosphate-buffered saline (PBS), freed of tendons and clumps of non-muscle tissue and chopped with scalpels into fragments <1 µL.
Mouse skeletal muscle tissue was collected from the legs of BALB/c or C57BL/6 (both strains from Harlan, Venray, the Netherlands) mice, pooled and chopped with scalpels into fragments measuring <1 µL.
Both human and mouse muscle mince was divided in aliquots of 250 µL and either cryopreserved or freshly implanted within 3 hours after collection.
The minced tissue aliquots used for preservation were suspended in culture medium (see next section) containing 20% dimethylsulfoxide (DMSO; Sigma-Aldrich, St. Louis, MO) and subjected to a slow freezing protocol. The frozen samples were stored in nitrogen vapor until use.

Isolation and culture of MSCs

hMSCs were isolated from bone marrow (BM) of a 38-year-old female undergoing orthopedic surgery. The BM sample was collected with a written informed consent and according to the guidelines of the LUMC. Cells were isolated and cultured as previously described[11]. Cell expansion was performed in culture medium consisting of Dulbecco's modified Eagle's medium (DMEM) containing 4.5 g/l glucose, L-glutamine, sodium pyruvate, 100 U/ml penicillin, 100 µg/ml streptomycin, and 10% fetal bovine serum (FBS) (all from Invitrogen, Breda, the Netherlands) and 0.5 ng/ml basic fibroblast growth factor (FGF2; Sigma-Aldrich) in CELLSTAR cell culture flasks (Greiner Bio-One, Frickenhausen, Germany) at 37°C in humidified air containing 10% CO_2.
mMSCs were isolated from BM of BALB/c female mice and cultured under the same conditions as the hMSCs.
hMSCs at passage number 4 and mMSCs at passage number 6 were tagged with LV.EF1a.CMV.LacZ as previously described[2].
The tumorigenic potential of mMSCs of passage 14 was tested through subcutaneous injection of 10^6 cells in NOD/SCID mice. Animals sacrificed at 15 and 36 days did not show any macroscopic alterations in primary organs and did not display abnormally growing cell masses at the site of injection.

Animals and subcutaneous implants

Recipient mice for the human and BALB/c mouse muscle mince were NOD/LtSz-scid/scid/J (NOD/SCID mice), initially purchased from Jackson Laboratory (Bar Harbor, ME). The possible contribution of host cells to the regeneration of subcutaneous skeletal muscle implants was studied using mice of which almost all tissues including skeletal muscle expressed a recombinant *enhanced green fluorescent protein* (*eGFP*) gene. These so-called C57BL/6-Tg (CAG+EGFP) C14-Y01-FM131Osb[12] mice received donor tissue from C57BL/6 mice. All mice were bred and maintained at the Animal Facility of the LUMC following the internal guidelines[13]. Experimentation with animals was performed in compliance with a protocol approved by the animal ethics committee of the LUMC.

Minced muscles of either human or mouse origin were implanted subcutaneously on the back of the mouse (Figure 6.1). Routinely, each NOD/SCID mouse received two implants, one of human and one of murine origin, to minimize the effect of recipient-associated conditions. Grafting was performed under aseptic conditions and general anesthesia with isoflurane. The back of the mouse was shaved and rinsed with ethanol. Next, two longitudinal 1-cm incisions to the left and right of the spine were made with a scalpel. The incisions were enlarged using scissors dissecting the skin from dorsal fascia thus forming a dermal pocket in which a standard volume of 250 µL minced skeletal muscle tissue alone or thoroughly mixed with 5×10^5 MSCs in 30 µL was inserted. The wound was closed with two or three ETHICON PROLENE polypropylene size 5-0 sutures (Johnson & Johnson Medical, Amersfoort, the Netherlands). After 7, 15, 30 or 45 days mice were sacrificed by cervical dislocation, the implants were removed and processed for (immuno)histological analyses.

Tissue processing and (immuno)histochemistry

The excised implants were cut in two halves and fixed either overnight at 4°C or for 1 hour at room temperature in 4% formaldehyde (Mallinckrodt Baker, Phillipsburg, NJ). Tissues fixed at room temperature were stained with 5-bromo-4-chloro-3-indolyl β-D-galactopyranoside (X-gal; Sigma-Aldrich) as previously described[2]. All samples were embedded in paraffin, cut into 6-µm-thick sections and placed on SuperFrost Plus slides (Menzel-Gläser, Braunschweig, Germany) for histochemical and immunohistological stainings.

Tissue sections of each sample were deparaffinized, rehydrated with graded ethanol-water mixtures and stained with hematoxylin, phloxin and saffron (HPS) following standard procedures. The slides were mounted with Pertex mounting medium (Histolab Products, Gothenburg, Sweden).

For immunohistology, tissue sections were deparaffinized, rehydrated and boiled 10 min in 10 mM citrate buffer (pH 6.0) for antigen retrieval. After rinsing the slides with water, endogenous peroxidase was inactivated by a 10-min incubation at room temperature with 0.3% (w/w) hydrogen peroxide in water. Following two additional washings with PBS a 1-h blocking step was performed using 10% goat serum (Dako Netherlands, Heverlee, Belgium) in PBS. Next, mouse monoclonal antibodies specific for human desmin (clone D33; IgG1, κ; Dako Netherlands, dilution 1:100) or directed against chicken Pax7 (IgG1, κ; Developmental Studies Hybridoma Bank, University of Iowa, Iowa City, IA; dilution 1:20) or the rabbit polyclonal anti-human von Willebrand factor (vWF) antiserum (Dako Netherlands; dilution 1:3,000) were added to sections for an overnight incubation at 4°C. The following day, the sections were washed in PBS and the secondary antibodies, either horseradish peroxidase-linked goat anti-mouse IgG (Dako Netherlands; dilution 1:100) or horseradish peroxidase-conjugated goat anti-rabbit IgG (Dako Netherlands; dilution 1:50) were applied for 30 min. The binding of the antibodies was visualized with 3,3'-diaminobenzidine (Sigma-Aldrich). The sections were counterstained with hematoxylin and mounted with Pertex mounting medium Images were captured with a Color View IIIu camera mounted on an Olympus BH-2 microscope and processed using Cell F-imaging software (all from Olympus Nederland, Zoeterwoude, the Netherlands).

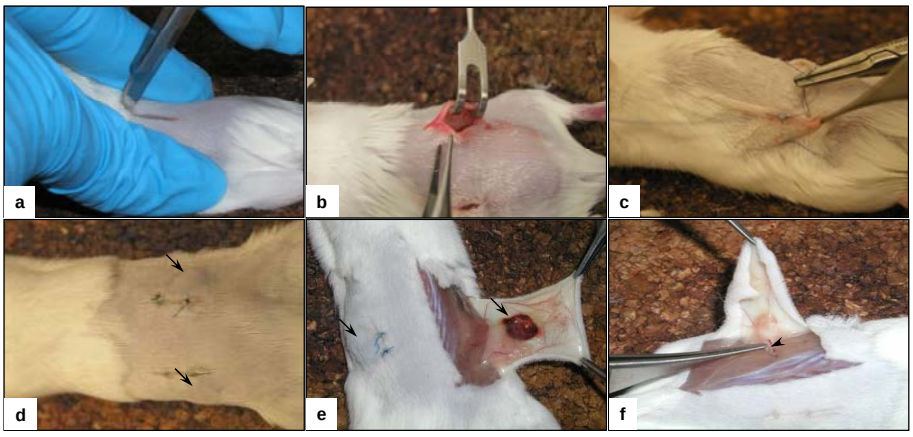

Figure 6.1 **Implantation procedure and macroscopic appearance of subcutaneous implants.** (a, b and c) Dorsal skin of NOD/SCID mouse showing incision, "pocket for the implant" and sutures, respectively. (d, e and f) Removal of implant at day 14. Arrows indicate implants and arrowhead a supplying blood vessel that was attached to the excised implant.

For the detection of eGFP-positive satellite cells an eGFP-specific rabbit polyclonal antiserum was used together with the aforementioned murine anti-Pax7 monoclonal antibody. Deparaffinized and rehydrated tissue sections were immersed twice in 10 mM citric acid solution (pH 6.0) for 5 min at 90°C. Following cooling and washing steps the sections were blocked for 2 to 3 h with 4% IgG- and protease-free bovine serum albumin (Jackson ImmunoResearch Europe, Newmarket, United Kingdom) in PBS. Next, the sections were sequentially incubated with goat anti-mouse IgG (H+L) AffiniPure Fab fragment (MouseFab, Jackson ImmunoResearch; dilution 0.05 mg/ml) for 30 min, with the anti-Pax7 antibody overnight, with biotin-SP-conjugated AffiniPure goat anti-mouse IgG (H+L) (Jackson ImmunoResearch; dilution 1:20) for 45 min and with Cy3-conjugated streptavidin (Jackson ImmunoResearch, dilution 1:1,250) for 30 min. Each incubation step was followed by three rinses with PBS. The sections were re-blocked with MouseFab for 30 min and labeled overnight with eGFP-specific rabbit polyclonal antiserum (IgG fraction; Invitrogen; dilution 1:200) followed by Alexa488-linked donkey anti-rabbit IgG (H+L) antibodies (Invitrogen; dilution 1:200) for 1 hour. Next, the sections were stained for 10 min at room temperature with 1 µg/ml of Hoechst 33342 (Invitrogen) in PBS, washed thrice with PBS to remove excess dye and mounted in Vectashield mounting medium (Vector Laboratories, Burlingame, CA). Light microscopic analysis was performed with a Leica DM5500 B fluorescence microscope (Leica Microsystems, Rijswijk, the Netherlands). Images were captured with a CoolSNAP *K4* CCD camera (Photometrics, Tuscon, AZ) and archived using home-made software.

Evaluation of tissue sections

Sections of the subcutaneous implants were microscopically evaluated for their myoregenerative state using HPS, desmin and Pax7. To enable a comparison between samples and conditions, we used an arbitrary scoring system with values between 1 and 5, as specified in Table 6.1, for each of the following parameters.

HPS stain was used to visualize the morphology of distinct components of the implants including degenerated myofibers (identified by the absence of nuclei), myoblasts, regenerating myofibers (characterized by the presence of multiple central nuclei), adipose tissue, capillaries and connective tissue. The regenerating myofibers served to estimate the relative size of the regenerating area in the implant as designated in Table 6.1.

In sections labeled with the anti-desmin antibody newly formed myofibers and myoblasts could be distinguished from non-regenerating areas in the implant by their intense brown staining. These sections were also used to estimate the relative area of regeneration in the implant as specified in Table 6.1.

Pax7-positive cells were counted in two regenerating areas of each section.

The presence of MSCs in the implants and their incorporation in myofibers was studied using sections stained with X-gal.

Table 6.1 Score of skeletal muscle regeneration and of the MSCs contribution in ectopic skeletal muscle implants.

Score	HPS or desmin* Frequency myoblasts/myofibers	Pax7[&] Frequency positive cells	X-gal Positive cells/myofibers
1	Few /single	1-5	Single/no
2	Many /some	5-10	Clusters/no
3	Many / many	10-15	Clusters/some
4	>80% of the area	15-20	Clusters/small clusters
5	100% of the area	>20	Clusters/large clusters

Results

Regeneration of ectopically implanted minced human and mouse skeletal muscle tissue

In an initial experiment designed to set up the model, the regeneration kinetics of fresh human and BALB/C mouse skeletal muscle tissue mince implanted under the skin of NOD/SCID mice were compared. The excised implants were screened for the presence of necrotic fibers, satellite cells, myoblasts and multinucleated myofibers.

In all cases the histological images (Figure 6.2) showed encapsulated implants isolated from their surroundings by dense connective tissue (identified by the yellow-orange saffron stain). HPS and desmin staining showed that the central part of the implants generally consisted of degenerating skeletal muscle tissue as evinced by the presence of anuclear myofibers. Myoregeneration typically started at the periphery of the implants, progressing with time towards the center. Myofibers were positioned in all directions (Figure 6.2Bc and f). Small blood vessels and capillaries (staining positive for the endothelial cell marker vWF; Figure 6.3) were initially (i.e. at 7 days after grafting) only found in the periphery of the implants but with time penetrated the inner parts.

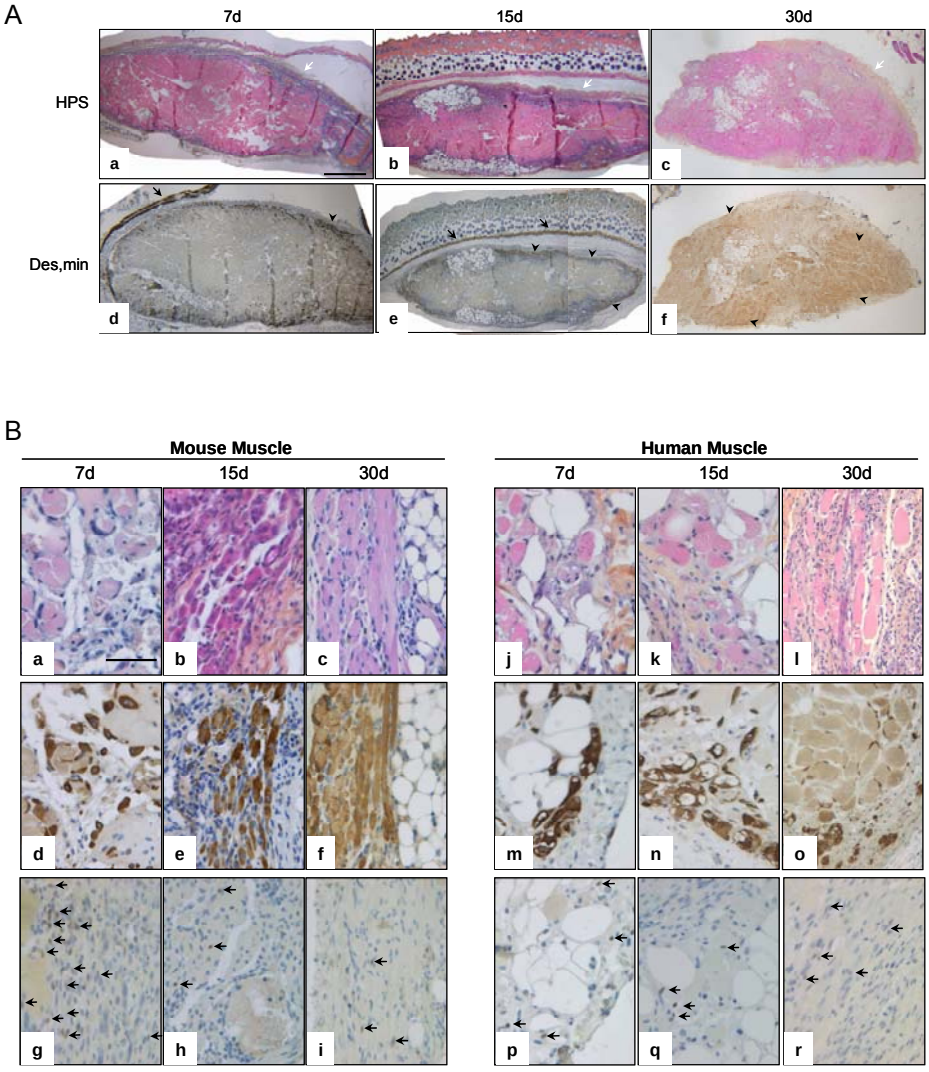

Figure 6.2 **Histological analysis of subcutaneous skeletal muscle implants.**
A: HPS- (upper panels) and desmin-stained (bottom panels) sections of fresh mouse muscle implants collected at 7 (a and d), 14 (b and e) and 30 (c and f) days after transplantation. Note that each implant is surrounded by a capsule staining yellow-orange by Saffron (white arrow in a, b and c). The intense brown desmin staining (d and e) portray the healthy myofibers of the panniculus carnosus of the host (black arrows in d and e) and myoblasts/regenerated myofibers of the implants (black arrowheads in d, e and f). Magnification: 20×. B: Two-hundred fold magnification of mouse (left panels) and human (right panels) implants excised at different time points. The sections were stained with HPS (upper panels), for desmin (middle panels) and for Pax7 (bottom panels). Arrows indicate Pax7+ cells. Magnification: 200×.

In the *mouse* muscle implants, shortly after transplantation (day 7), the thin peripheral rim of regenerated tissue consisted predominantly of mononucleated myoblasts (Figure 6.2Ba and d). Progression of the regenerative process was evident by the occurrence of elongated myofibers at days 15 and 30 post transplantation. The regenerating area gradually extended to occupy up to 80% of the implants at day 30 after transplantation (Figure 6.2Ac and f, 6.4 and 6.5). Satellite cells positive to Pax7 were detected in all implants, mostly in the periphery (Figure 6.2Bg, h and i). Their frequency in murine donor tissue was highest at day 7 and at day 45 after implantation (Figure 6.6). The observed decrease in the number of $Pax7^+$ cells at days 15 and 30 coincided with an increase in myoregeneration, suggesting that the first wave of these cells represents satellite cells mobilized from the implanted skeletal muscle tissue in response to the initial injury. If so, the second wave of $Pax7^+$ cells may represent their progeny that has been activated to support the ongoing regeneration.

The regeneration process in the *human* muscle implants resembled that in the murine muscle implants albeit with a slower progression (Figure 6.2B). The frequency of myoblasts and regenerated myofibers scored in the human tissue at day 30 after implantation was in the same range at that in the murine muscle at day 7 post transplantation. Regeneration in the human tissue still continued at day 45 after implantation, the last time point analyzed (Figure 6.4 and 6.5). The latter observation together with the high number of satellite cell scored at 45 days (Figure 6.6) suggests that regeneration of the human muscle implants has not yet reached its peak at this time point.

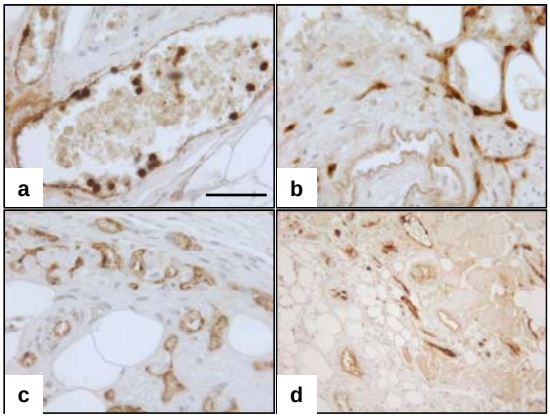

Figure 6.3 **Vascularization of subcutaneous skeletal muscle implants.**
Shown are photomicrographs of sections of fresh human (a and b) and mouse (c and d) minced muscle implants collected at 30 days after transplantation and stained with a vWF-specific antibody to visualize capillaries and blood vessel (brown stain). Magnification: 400×.

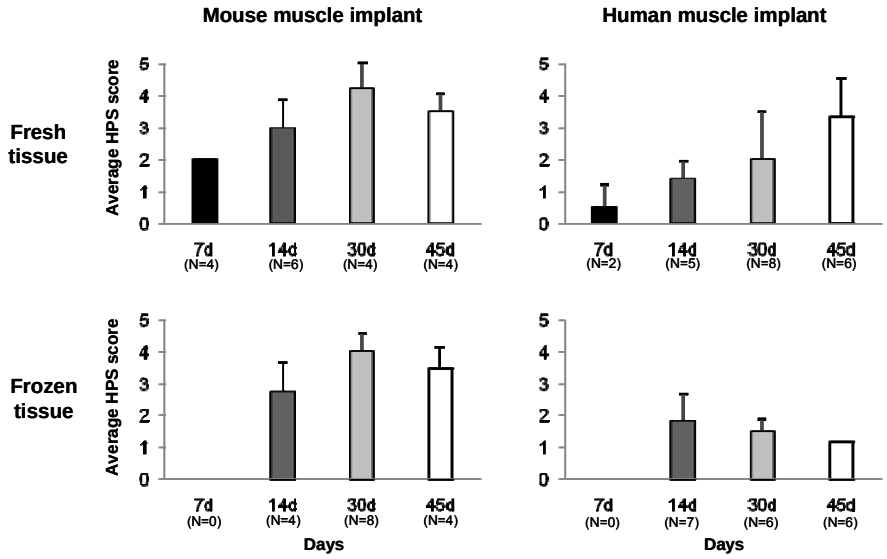

Figure 6.4 **Myoregeneration of skeletal muscle implants as scored by HPS staining.** Sections of minced muscle implants were excised at different time points, stained and evaluated microscopically. Average score and standard deviation (SD) are plotted. N represents the number of implants analyzed.

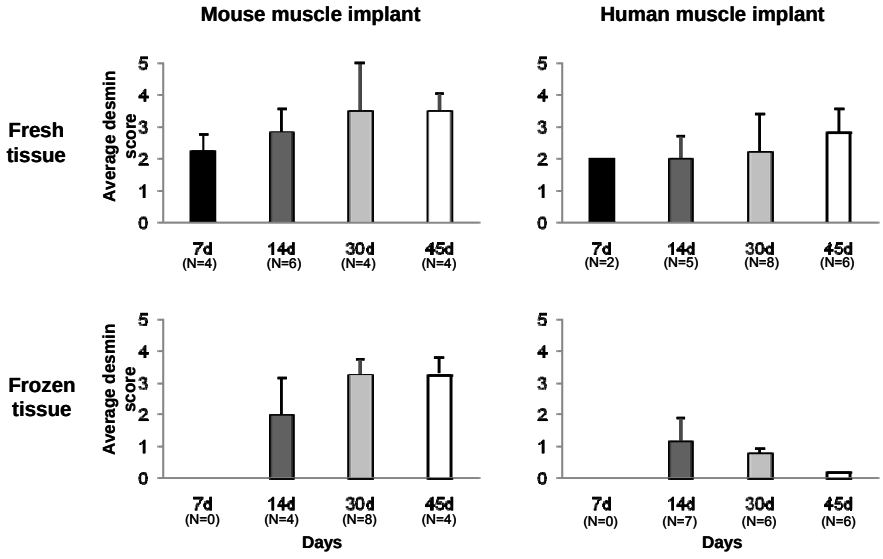

Figure 6.5 **Myoregeneration of skeletal muscle implants as scored by desmin staining.** Sections of minced muscle implants were excised at different time points, stained and evaluated by microscopy. Average score and SD are plotted. N represents the number of implants analyzed.

Regeneration of cryopreserved skeletal muscle tissue

Due to the irregular supply of human skeletal muscle samples and their limited size (sufficient for only one and occasionally two implants per donor), we explored the option of implanting minced skeletal muscle tissue that had been cryopreserved allowing us to pool skeletal muscle samples from multiple donors. By this approach one might also expect to improve reproducibility.
The regeneration of cryopreserved *mouse* skeletal muscle implants closely resembled that of the fresh implants as judged by HPS and desmin staining and by the frequency of $Pax7^+$ cells (Figure 6.4, 6.5 and 6.6). *Human* skeletal muscle tissue cryopreserved in an identical manner responded differently. At 14 days after transplantation, ingrowth of capillaries and signs of myoregeneration were observed at the edges of the donor tissue like in implants of fresh tissue but at later time points (days 30 and 45), the implants of tissue that had been frozen were composed mostly of loose connective and adipose tissue. The number of satellite cells in the human skeletal muscle tissue that had been cryopreserved clearly decreased from day 14 onwards suggesting deterioration of this cell population (Figure 6.6).

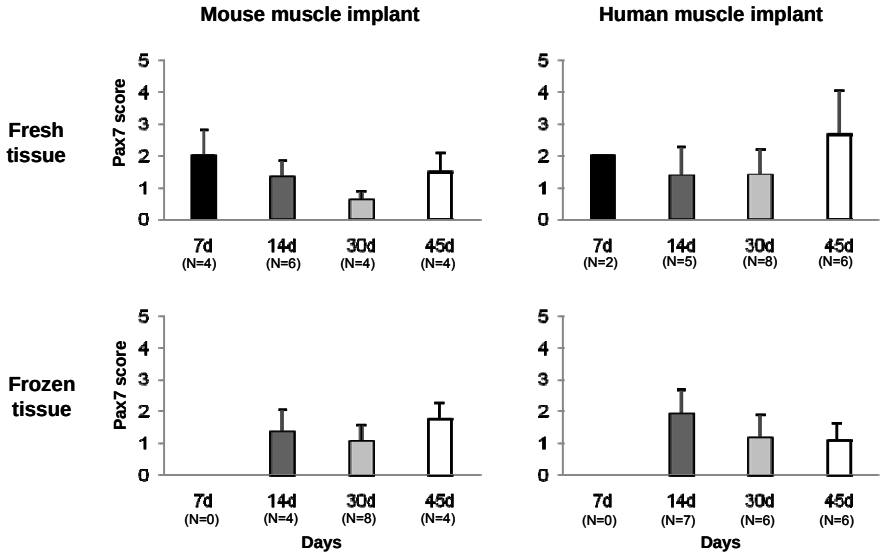

Figure 6.6 **Satellite cell counts in regenerating skeletal muscle implants**.
Mouse and human implants of fresh or cryopreserved minced muscle tissue were excised at different time points, processed for immunohistochemistry and analyzed for the presence of Pax7+ cells. Average score and SD are plotted. N represents the number of implants analyzed.

Contribution of host cells to myoregeneration in subcutaneous skeletal muscle implants

The skin of a mouse, like that of most rodents, contains a thin muscle layer named the *panniculus carnosus*. As some damage of the *panniculus carnosus* during the implantation procedure is unavoidable, a possible contamination of the graft with recipient satellite cells has to be taken in consideration. This was investigated using *eGFP*-expressing transgenic hosts that were implanted with skeletal muscle tissue of syngeneic C57BL/6 mice. The minced muscle implants were analyzed 7 days later for the presence of $eGFP^+$ cells expressing *Pax7* indicative of host-derived satellite cell contribution. A large number of $eGFP^+$ mononucleated cells was present in the implants but only a few isolated cells co-expressed *Pax7* (Figure 6.7). Also present were a few $eGFP^+$ myofibers at the periphery of the implants (Figure 6.7). These findings demonstrate a negligible contribution of recipient cells to the myoregenerative process in the implants and are in agreement with previous reports[9,21].
The evident profusion of donor-derived mononuclear cells in the implants, representing infiltration of blood-derived granulocytes and monocytes, underlines the functional vascularization of the graft already at an early time point after transplantation.

Contribution of syngeneic or xenogeneic MSCs to myoregeneration in subcutaneous skeletal muscle implants

Addition of BM-derived *LacZ*-tagged MSCs of either mouse or man to minced skeletal muscle tissue (fresh or cryopreserved; see Figure 6.8) prior to implantation did not consistently affect the degree or kinetics of myoregeneration to any significant extent. The persistence of mMSCs and their participation in myofiber formation were similar for the fresh and cryopreserved *murine* skeletal muscle samples. In contrast, hMSCs were strikingly less abundant in the implants of fresh *mouse* muscle tissue than in those containing minced *mouse* muscle that had been cryopreserved (Figure 6.9A and B). Also different was the distribution of the human and mouse MSCs in the implants of cryopreserved *murine* muscle. The mouse cells were concentrated in the periphery of the implants, while the human cells were distributed throughout the grafts (Figure 6.9C).
The effects of mixing *human* skeletal muscle samples with MSCs on subsequent implant regeneration could only be investigated using donor material that had been cryopreserved. Supplementation of the human muscle mince with either mMSCs or hMSCs did not lead to the formation of $\beta\text{-gal}^+$ (i.e. hybrid) myofibers at any of the time points analyzed. Under all conditions, the MSCs were maintained in the implants as isolated or clustered mononuclear cells (Figure 6.10).

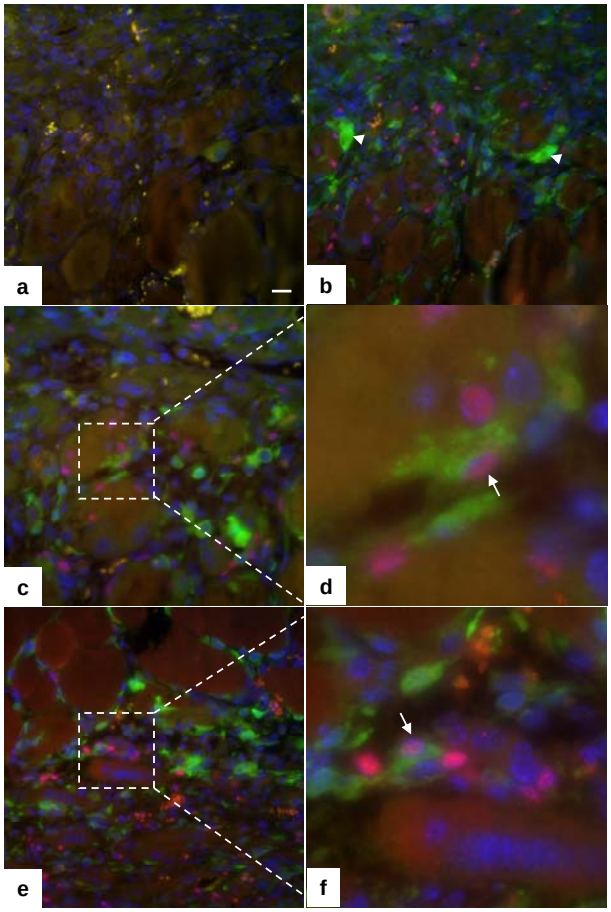

Figure 6.7 **Contribution of host cells to myoregeneration in the implant**.
Immunofluorescence analysis of fresh mouse (C57BL) muscle tissue excised 7 days after implantation on a back of an eGFP transgenic recipient. Host cell contribution was evaluated in sections stained with antibodies specific for eGFP and Pax7. (a) Negative control consisting of tissue section exclusively incubated with secondary antibodies and Cy3-conjugated streptavidin. (b) Tissue section stained for Pax7 (red), eGFP (green) and with the karyophilic fluorochrome Hoechst 33342 (blue). Arrowheads indicate GFP+ myofibers located at the periphery of the implant. (c and e) Examples of cells positive for both Pax7 and eGFP (arrows) situated at the periphery of the implant (Magnification: 400×) and their electronic enlargements (d and f).

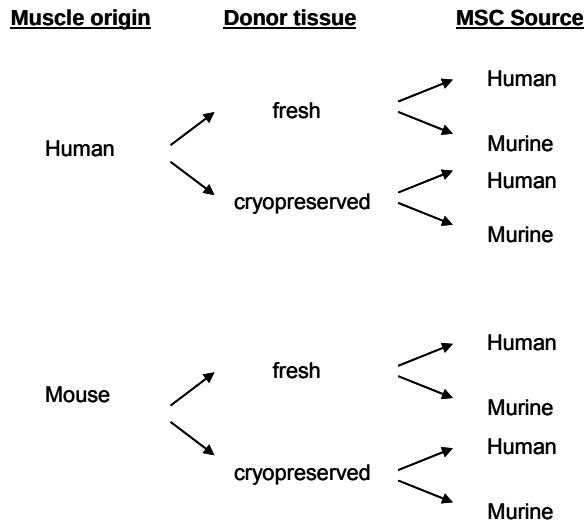

Figure 6.8 Schematic presentation of the experiments in which minced skeletal muscle tissue of human or murine origin was mixed with mMSCs or hMSCs prior to subcutaneous implantation into NOD/SCID mice.

A

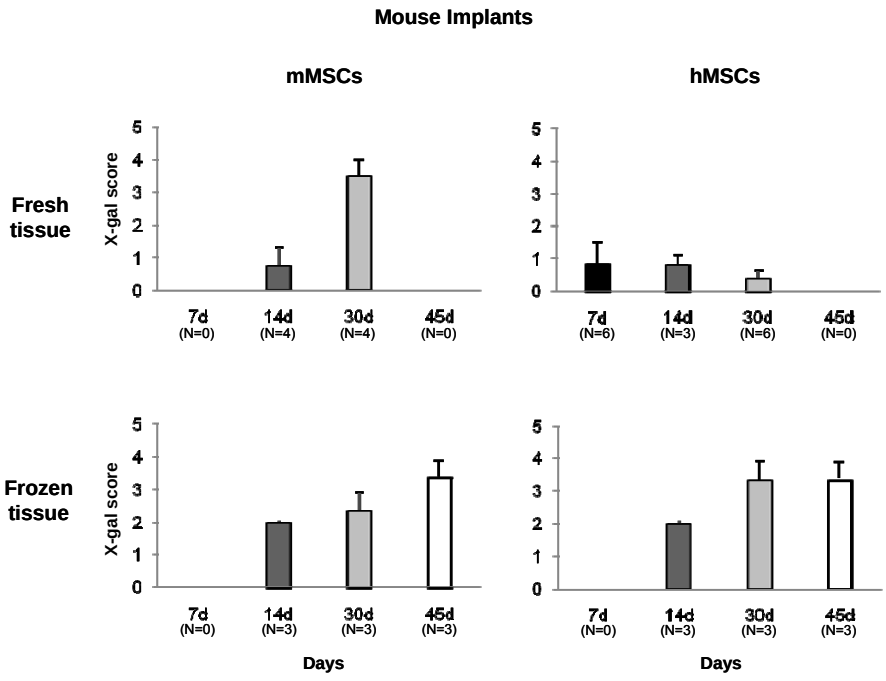

B

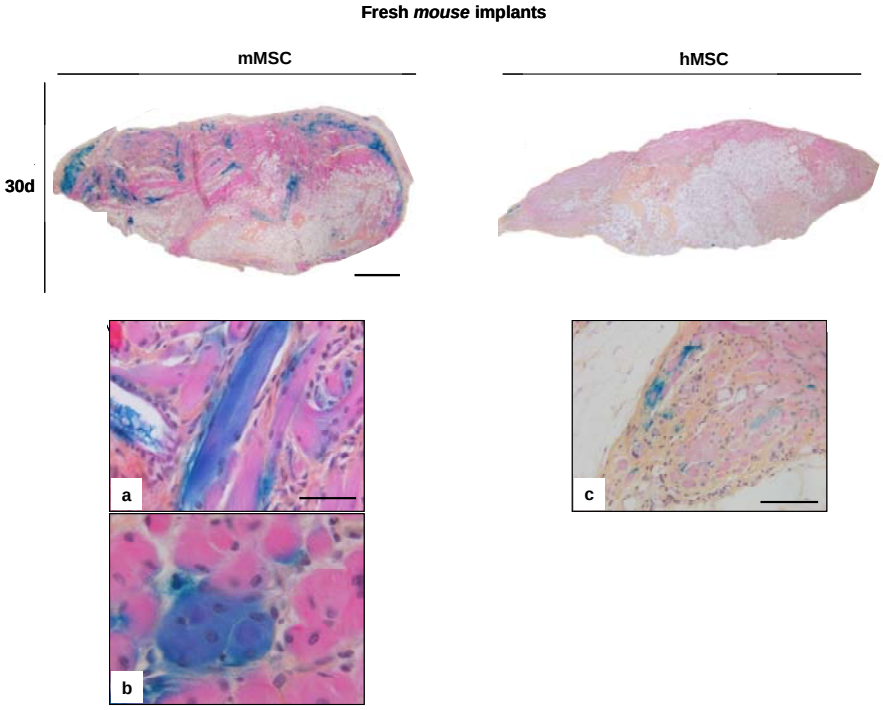
Fresh *mouse* implants
mMSC
hMSC
30d
a
b
c

C

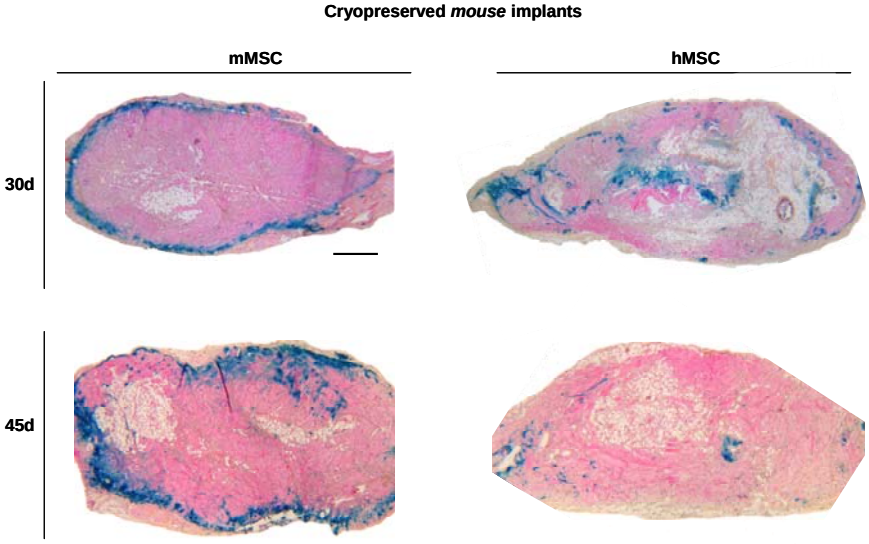
Cryopreserved *mouse* implants
mMSC
hMSC
30d
45d

D

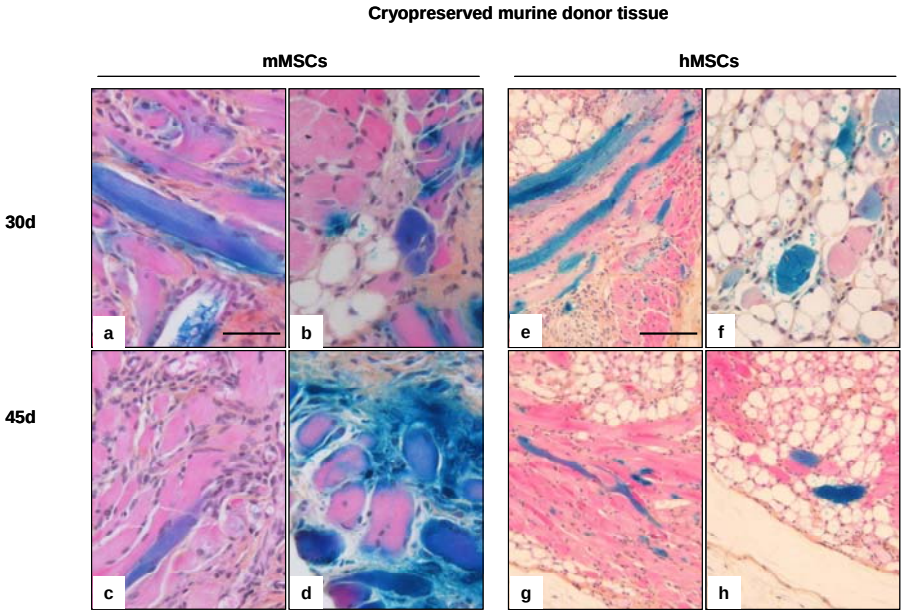

Figure 6.9 **Contribution of mMSCs and hMSCs to myoregeneration in implants of fresh and cryopreserved mouse skeletal muscle.** MSCs and there derivatives were identified by X-gal staining. A: Grafts of fresh and cryopreserved minced muscle mixed with mMSCs or hMSCs were excised at different time points and evaluated for the presence of β-gal+ mononuclear cells and myofibers. Average of X-gal scores and SD are plotted. N represents the number of implants analyzed. B: X-gal-stained sections of fresh mouse muscle implants removed 30 days after grafting. Notice the higher frequency of blue myofibers in the implants containing mMSCs (a and b) as compared to those with hMSCs (c). Magnifications: 20× (upper panels), 400× (a and b), 200× (c). C: X-gal-stained sections of cryopreserved mouse muscle implants excised at 30 and 45 days post transplantation. Magnification: 20×. D: Higher magnification of sections showed in C. (a, b, c and d) β-gal+ mononuclear cells and myofibers (longitudinal and transversal cuts) at 30 and 45 days after transplantation in implants with mMSCs. Magnification: 400×. (e, f, g and h): β-gal+ myofibers (longitudinal and transversal cuts) and few β-gal+ mononuclear cells in tissues supplemented with hMSCs that were excised 30 and 45 days after implantation. Magnification: 200×.

A

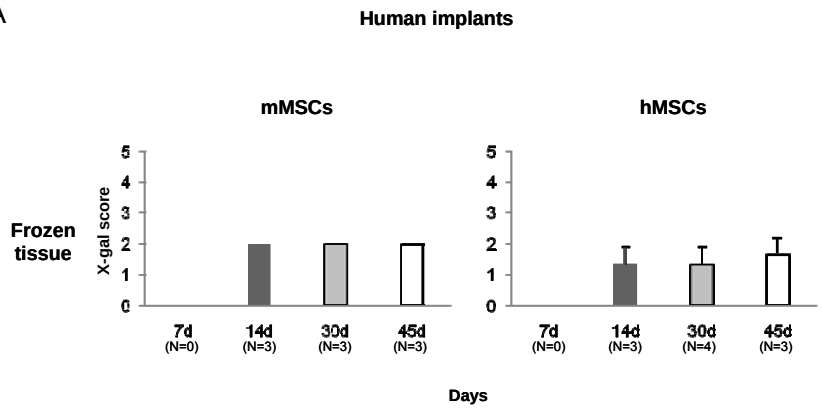
Human implants
mMSCs
hMSCs
Frozen tissue
X-gal score
0
1
2
3
4
5
7d (N=0)
14d (N=3)
30d (N=3)
45d (N=3)
7d (N=0)
14d (N=3)
30d (N=4)
45d (N=3)
Days

B

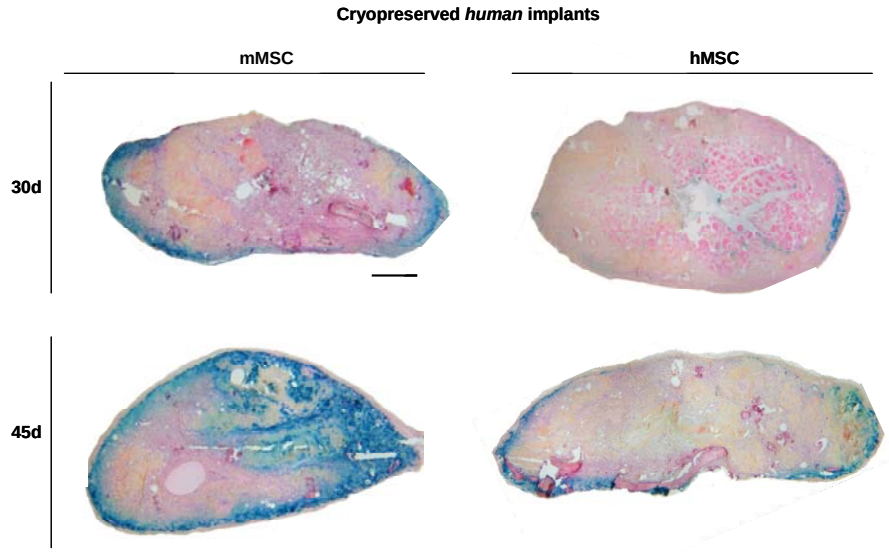
Cryopreserved *human* implants
mMSC
hMSC
30d
45d

C

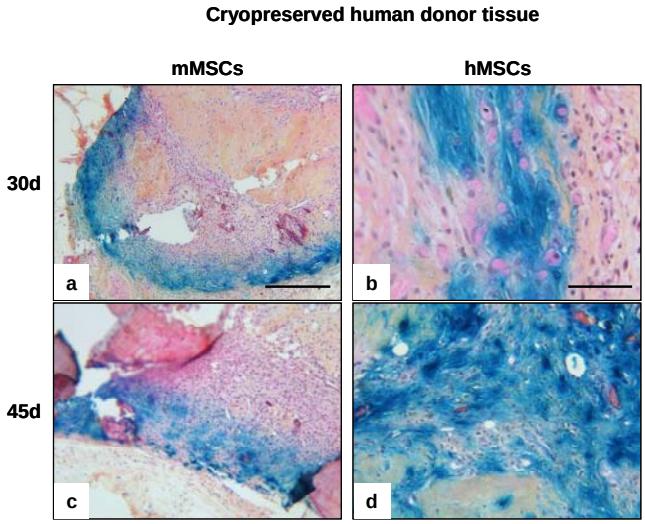

Figure 6.10 **Contribution of mMSCs and hMSCs to myoregeneration in implants of cryopreserved human skeletal muscle.** MSCs and there derivatives were identified by X-gal staining. A: Grafts of cryopreserved minced muscle mixed with mMSCs or hMSCs were excised at different time points and evaluated for the presence of β-gal+ mononuclear cells and myofibers. Average of X-gal scores and SD are plotted. N represents the number of implants analyzed. B: Photographs of X-gal-stained whole-mount sections of implants excised at days 30 and 45 post transplantation. Magnification: 20× C: Two-hundred fold magnification of sections showing β-gal+ cells but no blue myofibers.

Discussion

A major impediment to the development of stem cell therapy for myogenic disorders is the paucity of reliable animal models for regenerating human skeletal muscle. Our endeavor to develop a model that comprises immunodeficient mice as recipients of subcutaneously implanted human skeletal muscle fragments. Although engraftment of minced human muscle tissue could be demonstrated, several obstacles were encountered, the major one being the inadequate supply of human muscle tissue. We attempted to overcome this problem by cryopreservation and banking of the human samples prior to their implantation. However, the DMSO-mediated freezing procedure proved to be destructive for the satellite cells thereby precluding regeneration. This difficulty was not encountered with murine muscle mince. Regeneration of the murine skeletal muscle samples that had been cryopreserved progressed similarly to that of fresh muscle specimens. The different response of human and murine skeletal muscle tissue to cryopreservation was rather unexpected especially in view of an earlier study by Liveson et al.[14] who employed a similar

freezing procedure (with a lower concentration of DMSO: 7% versus 20%) and validated tissue recovery in organotypic tissue culture. These authors reported the absence of significant ultrastructural or electrophysiological differences between muscle implants which regenerated from previously frozen or unfrozen tissues of both human and mouse origin. Nonetheless, morphological and immunohistological comparison of murine and human fresh muscle implants support the potential of our model as a platform for studying skeletal muscle regeneration.

The myoregeneration of the human muscle implants resembles largely that of the murine implants. Both tissues were encapsulated, vascularized and infiltrated by host-derived blood cells. The kinetics of myoregeneration was, however, different. While in the murine tissue satellite cell counts were highest at day 7 and the area of regeneration reached up to 80% of the total implant at day 30 after transplantation, in the human implants satellite cells numbers peaked at day 45 with only 20% of the implant showing signs of myoregeneration. The evident elevation in satellite cell numbers at day 45 suggests, in analogy to the situation with the murine muscle samples, that full regeneration of the human implants has not been achieved at this time point. The emerging pattern of mouse implants regenerating faster than their human counterparts is in line with the general rule that the larger the animal the longer the myoregeneration process[15].

The irregular supply of human skeletal muscle tissue impeded in particular the studies involving addition of MSCs with its complicated logistics. The interaction between MSCs (murine and human) and the regenerating tissue could, therefore, only be assessed for fresh and cryopreserved murine skeletal muscle and for cryopreserved human skeletal muscle.

The observation that the addition of MSCs has little or no effect on the rate of myoregeneration corroborates previous findings from our research group with human BM-derived MSCs and cardiotoxin (CTX)-injured murine muscles[2].

The contribution of MSCs to myofiber formation, as visualized by X-gal staining, seems to occur only in tissues undergoing massive myoregeneration like in the murine implants at 30 and 45 days post transplantation. In tissues with low or no evident regeneration, as in the cryopreserved human muscle implants at day 30 after transplantation, β-gal$^+$ myofibers were not detected. The dependency of β-gal$^+$ myofiber appearance on ongoing regeneration in close vicinity of the donor cells was also observed in CTX-damaged muscles that were depleted of satellite cells by irradiation (our unpublished observation). Although the damaged skeletal muscle tissue in both models (CTX-treated muscle and minced tissue implants) provides proper myogenic stimuli, myoregeneration does not seem to progress in the absence of satellite cells. The observation that MSCs are maintained in these environments as mononucleated cells without contributing to the satellite cell pool or forming

homotypic myofibers may argue against them having autonomic myogenic differentiation capacity. The β-gal$^+$ myofibers observed in the murine implants might then arise solely by fusion of MSCs with nascent or regenerating implant-derived myofibers during the regeneration process.

Differences in the participation of syngeneic versus xenogeneic MSCs in myoregeneration of the fresh *mouse* muscle implant were observed at 30 days after grafting (Figure 6.9A). The 3-fold higher contribution of the mMSCs as compared to the hMSCs is in line with findings in the CTX-damage model of the *tibialis anterior* muscle where hMSCs were half as effective in the production of β-gal$^+$ myofibers as mMSCs (average 45±16.2 and 27±18.3 respectively; our unpublished data). Although it may not be fully appropriate to compare these models in view of the different forms of injury. More interesting was the finding that the level of participation of hMSCs equaled that of mMSCs when the mouse skeletal muscle mince had been cryopreserved prior to implantation. It is tempting to speculate that this indicates the presence of species-specific inhibitors in the mouse tissue that become inactivated by the cryopreservation. This model offers excellent opportunities for identifying such inhibitors and evaluating their significance for cell therapy.

The notion that the differentiation potential of MSCs is restricted to osteoblasts, chondrocytes, adipocytes, fibroblasts and adventitial reticular cells gained recently much support[16]. Evidence regarding the ability of MSCs to differentiate along the myogenic line is conflicting. Although some previous studies assigned myogenic properties to MSCs by demonstrating their *in vitro* and *in vivo* differentiation into satellite cells and myoblasts and their homotypic cell fusion[17,18], others regard the myogenic reprogramming of the MSCs to be a consequent of their fusion with inherently myogenic cells[2,19,24,25]. Whether this contradiction can be attributed to the differences in MSC origin, the model used or the read-out methods applied remains thus far unclear. The ability of the model based on ectopic frozen human muscle implant to distinguish genuine myodifferentiation from heterotypic cell fusion may help to clarify this inconsistency. It also renders this model most valuable for the screening of the therapeutic potential of other stem cell populations.

At 30 and 45 days after transplantation, the cryopreserved human muscle implants displayed histological features very similar to those of DMD patients' muscles in later stages of the disease[20,21]. Despite the different etiology (ischemia-reperfusion versus congenital muscle degeneration) the lack of satellite cells in both cases impedes myoregeneration leading eventually to replacement of the damaged muscle tissue with fibrotic and adipose tissue. This resemblance is worthy to be explored further for a better understanding of skeletal muscle degeneration and to create new prospects to reverse the process or intervene with its progression.

In summary, our primary question of whether the contribution of MSCs to myoregeneration is subject to species barriers could be partly answered through the use of ectopically implanted minced muscle. hMSCs were found not to participate in the regeneration of fresh mouse muscle implants and this inhibition was alleviated using muscle mince that had been cryopreserved prior to implantation. Collectively, our data indicate that the *in vivo* model described herein is valuable for studying different aspects of human skeletal muscle regeneration and degeneration which justify its further exploitation. The major issues to be tackled are the logistics of patient's tissue supply and the cryopreservation of human skeletal muscle specimens.

References

1. Dellavalle A, Sampaolesi M, Tonlorenzi R, Tagliafico E, Sacchetti B, Perani L, Innocenzi A, Galvez BG, Messina G, Morosetti R, Li S, Belicchi M, Peretti G, Chamberlain JS, Wright WE, Torrente Y, Ferrari S, Bianco P, Cossu G. Pericytes of human skeletal muscle are myogenic precursors distinct from satellite cells. Nat Cell Biol, 9:255-67, 2007.
2. de la Garza-Rodea AS, van der Velde I, Boersma H, Gonçalves MA, van Bekkum DW, de Vries AA, Knaän-Shanzer S. Long-term contribution of human bone marrow mesenchymal stromal cells to skeletal muscle regeneration in mice. Cell Transplant, 20:217-31, 2011.
3. Bouchentouf M, Benabdallah BF, Mills P, Tremblay JP. Exercise improves the success of myoblast transplantation in mdx mice. Neuromuscul Disord, 16:518-29, 2006.
4. Ikemoto M, Fukada S, Uezumi A, Masuda S, Miyoshi H, Yamamoto H, Wada MR, Masubuchi N, Miyagoe-Suzuki Y, Takeda S. Autologous transplantation of SM/C-2.6$^+$ satellite cells transduced with micro-dystrophin *CS1* cDNA by lentiviral vector into *mdx* mice. Mol Ther, 15:2178-85, 2007.
5. Cerletti M, Jurga S, Witczak CA, Hirshman MF, Shadrach JL, Goodyear LJ, Wagers AJ. Highly efficient, functional engraftment of skeletal muscle stem cells in dystrophic muscles. Cell, 11;134:37-47, 2008.
6. Studitsky AN. Free auto- and homografts of muscle tissue in experiments on animals. Ann N Y Acad Sci, 30;120:789-801, 1964.
7. Grounds M, Partridge TA, Sloper JC. The contribution of exogenous cells to regenerating skeletal muscle: an isoenzyme study of muscle allografts in mice. J Pathol, 132:325-41, 1980.
8. Wakayama Y, Schotland DL, Bonilla E. Transplantation of human skeletal muscle to nude mice: a sequential morphologic study. Neurology, 30:740-8, 1980.
9. Grounds MD, Partridge TA. Isoenzyme studies of whole muscle grafts and movement of muscle precursor cells. Cell Tissue Res, 230:677-88, 1983.
10. Gulati AK, Rivner MH, Shamsnia M, Swift TR, Sohal GS. Growth of skeletal muscle from patients with amyotrophic lateral sclerosis transplanted into nude mice. Muscle Nerve, 11:33-8, 1988.
11. Knaän-Shanzer S, van de Watering MJ, van der Velde I, Gonçalves MA, Valerio D, de Vries AA. Endowing human adenovirus serotype 5 vectors with fiber domains of species B greatly enhances gene transfer into human mesenchymal stem cells. Stem Cells, 23:1598-607, 2005.
12. Okabe M, Ikawa M, Kominami K, Nakanishi T, Nishimune Y. 'Green mice' as a source of ubiquitous green cells. FEBS Lett, 407:313-9, 1997.
13. Knaän-Shanzer S, van der Velde-van Dijke I, van de Watering MJ, de Leeuw PJ, Valerio D, van Bekkum DW, de Vries AA. Phenotypic and functional reversal within the early human hematopoietic compartment. Stem Cells, 26:3210-7, 2008.
14. Liveson JA, Peterson ER, Crain SM, Borstein MB. Regeneration in vitro of previously frozen adult mouse and human striated muscle coupled with fetal spinal cord. Exp Neurol, 48:624-36, 1975.
15. Carlson BM. The biology of muscle transplantation, p. 3-18. In Muscle transplantation (Eds. Freilinger G, Holle J, Carlson BM), Springer-Verlag, Wien, 1981.
16. Bianco P, Robey PG, Simmons PJ. Mesenchymal stem cells: revisiting history, concepts, and assays. Cell Stem Cell, 2:313-9, 2008.
17. Liu Y, Yan X, Sun Z, Chen B, Han Q, Li J, Zhao RC. Flk-1$^+$ adipose-derived mesenchymal stem cells differentiate into skeletal muscle satellite cells and ameliorate muscular dystrophy in mdx mice. Stem Cells Dev, 16:695-706, 2007.
18. De Bari C, Dell'Accio F, Vandenabeele F, Vermeesch JR, Raymackers JM, Luyten FP. Skeletal muscle repair by adult human mesenchymal stem cells from synovial membrane. J Cell Biol, 160:909-18, 2003.
19. Bianco P, Robey PG, Saggio I, Riminucci M. "Mesenchymal" stem cells in human bone marrow (skeletal stem cells): a critical discussion of their nature, identity, and significance in incurable skeletal disease. Hum Gene Ther, 21:1057-66, 2010.

20. Carpenter S, Karpati G. Pathology of skeletal muscle, 2nd Ed. Oxford University Press, New York, 2001.
21. Banker BQ, Engel AG. Basic reactions of muscle, p. 691-747. In Myology, 1st Vol., 3rd Ed. (Eds. Engel AG, Franzini-Armstrong C), McGraw-Hill, New York, 2004.
22. Washabaugh CH, Ontell MP, Ontell M. Nonmuscle stem cells fail to significantly contribute to regeneration of normal muscle. Gene Ther, 11:1724-8, 2004.
23. Irintchev A, Rosenblatt JD, Cullen MJ, Zweyer M, Wernig A. Ectopic skeletal muscles derived from myoblasts implanted under the skin. J Cell Sci, 111:3287-97, 1998.
24. Shi D, Reinecke H, Murry CE, Torok-Storb B. Myogenic fusion of human bone marrow stromal cells, but not hematopoietic cells. Blood, 104:290-94, 2004.
25. Gonçalves MA, Swildens J, Holkers M, Narain A, van Nierop GP, van de Watering MJ, Knaän-Shanzer S, de Vries AA. Genetic complementation of human muscle cells via directed stem cell fusion. Mol Ther, 16:741-48, 2008.